LETTERS

Control of the electronic phase of a manganite by mode-selective vibrational excitation

Matteo Rini[1], Ra'anan Tobey[2], Nicky Dean[2], Jiro Itatani[1,3], Yasuhide Tomioka[4], Yoshinori Tokura[4,5], Robert W. Schoenlein[1] & Andrea Cavalleri[2,6]

Controlling a phase of matter by coherently manipulating specific vibrational modes has long been an attractive (yet elusive) goal for ultrafast science. Solids with strongly correlated electrons, in which even subtle crystallographic distortions can result in colossal changes of the electronic and magnetic properties, could be directed between competing phases by such selective vibrational excitation. In this way, the dynamics of the electronic ground state of the system become accessible, and new insight into the underlying physics might be gained. Here we report the ultrafast switching of the electronic phase of a magnetoresistive manganite via direct excitation of a phonon mode at 71 meV (17 THz). A prompt, five-order-of-magnitude drop in resistivity is observed, associated with a non-equilibrium transition from the stable insulating phase to a metastable metallic phase. In contrast with light-induced[1–3] and current-driven[4] phase transitions, the vibrationally driven bandgap collapse observed here is not related to hot-carrier injection and is uniquely attributed to a large-amplitude Mn–O distortion. This corresponds to a perturbation of the perovskite-structure tolerance factor, which in turn controls the electronic bandwidth via inter-site orbital overlap[5,6]. Phase control by coherent manipulation of selected metal–oxygen phonons should find extensive application in other complex solids—notably in copper oxide superconductors, in which the role of Cu–O vibrations on the electronic properties is currently controversial.

Manganites exhibit a number of exotic phenomena, including charge-ordered and striped phases, orbital and magnetic ordering, half-metallicity, phase separation and colossal magnetoresistance[5,6]. Most of these phenomena stem from the strong interaction between lattice, charge, orbital and spin degrees of freedom, which compete on similar energy scales to determine the ground state of the system[7]. Arguably, the most striking aspect of the physics of manganites is the occurrence of a number of metal–insulator transitions, initiated for instance via perturbations of temperature, magnetic field, pressure and irradiation with light[5].

$Pr_{1-x}Ca_xMnO_3$ is a unique example among manganites, exhibiting insulating behaviour over the entire chemical composition x and over the entire temperature range[8]. This is a consequence of the small ionic radius of Ca, which results in a pronounced orthorhombic distortion (Fig. 1a) that favours charge localization[6]. Notably, the insulating phase at $x = 0.3$ adjoins a 'hidden' metallic state of the system, characterized by enormous changes in resistivity.

In ABO_3 perovskites, the orthorhombic distortion is quantified by the geometric 'tolerance factor' that depends on the average A–O (A = Pr, Ca) and B–O (B = Mn) distances:

$$\Gamma = \frac{(A-O)}{\sqrt{2}(B-O)}$$

where $\Gamma = 1$ corresponds to an ideal cube, while $\Gamma < 1$ reflects a compression of the Mn–O bond and an elongation of the A–O bond. Moreover, $\Gamma < 1$ indicates a Mn–O–Mn angle θ that is smaller than 180°, consistent with a symmetry-lowering rotation leading to orthorhombic or rhombohedral structures. The tolerance factor is related to the electronic properties of the solid via the one electron bandwidth W, because the capacity for $3d$ electrons to hop between neighbouring Mn-atoms depends on a super-transfer process via O($2p$) states and on the degree of overlap between orbitals in neighbouring sites[6,9,10]. The hopping matrix element reaches its maximum at $\theta = 180°$ (cubic), and decreases with θ, vanishing at $\theta = 90°$. Systematic studies of several $A_{0.7}A'_{0.3}MnO_3$ compounds show that the tolerance factor controls the competition between ferromagnetic metallic, paramagnetic insulating, and ferromagnetic insulating phases[11].

Here we show that coherent excitation of specific infrared-active modes can control the electronic phase of a manganite via direct modulation of the tolerance factor. Figure 1b shows the low-temperature optical conductivity spectrum of $Pr_{0.7}Ca_{0.3}MnO_3$ with three dominant

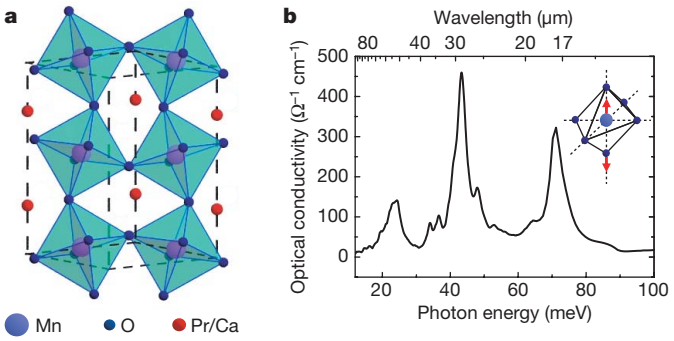

Figure 1 | $Pr_{0.7}Ca_{0.3}MnO_3$ crystal structure and vibrational spectrum. **a**, Unit cell of $Pr_{0.7}Ca_{0.3}MnO_3$ with pronounced orthorhombic distortion resulting from the small ionic radius of the Ca atoms. The Mn–O–Mn bond is bent at an angle $\theta < 180°$, which varies linearly with the tolerance factor Γ (ref. 10). The Pr/Ca doping results in an alternating network of Mn^{3+} and Mn^{4+} ions. The crystal field splits the fivefold Mn $3d$ levels into t_{2g} and e_g subsets. The electron hopping occurs between $3d$ e_g levels of neighbouring Mn^{3+} and Mn^{4+} species. The lattice distortion is related monotonically to the one electron bandwidth W, because the effective hopping interaction of $3d$ electrons between neighbouring Mn sites depends on super-transfer process via O($2p$) states, and the p-orbital of oxygen cannot point towards two manganese atoms simultaneously if $\theta \neq 180°$ (ref. 6). **b**, Low-temperature (10 K) optical conductivity spectrum of $Pr_{0.7}Ca_{0.3}MnO_3$. The inset shows the atomic displacements within the MnO_6 octahedra associated with the 71 meV phonon mode that modulates the Mn–O distance, and hence the tolerance factor.

[1]Materials Sciences Division, Lawrence Berkeley National Laboratory, Berkeley, California 94720, USA. [2]Department of Physics, Clarendon Laboratory, University of Oxford, Oxford OX1 3PU, UK. [3]ERATO, Japan Science and Technology Agency, Chiyoda-ku, Tokyo 102-0075, Japan. [4]Correlated Electron Research Center, AIST, Tsukuba, Ibaraki, 305-8562 Japan. [5]Department of Applied Physics, University of Tokyo, Tokyo 113-8656, Japan. [6]Central Laser Facility, Rutherford Appleton Laboratory and Diamond Light Source, Chilton, Didcot, OX11 0QX, UK.

phonon modes (23, 42 and 71 meV)[12] corresponding to the three (F_{2u}) infrared active vibrational modes of a cubic perovskite. The orthorhombic distortion is responsible for the appearance of a number of weaker resonances, although only a subset of the active 25 ($7B_{1u} + 9B_{2u} + 9B_{3u}$) infrared phonon modes of a *Pbnm* orthorhombic structure is clearly visible. The two highest-frequency vibrations are assigned to the Mn–O–Mn bending mode and the Mn–O stretching mode respectively[13]. Both vibrational modes affect the geometrical parameters determining the tolerance factor and are thus expected to have a strong coupling to the electronic properties of the system. Here we focus on the highest-frequency Mn–O stretching vibration at 71 meV and study the effect of coherent large-amplitude excitation of this mode with intense femtosecond mid-infrared pulses. The material response is investigated using both ultrafast pump–probe spectroscopy and transient conductivity measurements to characterize the insulator–metal transition[2,3,14–17].

$Pr_{1-x}Ca_xMnO_3$ single crystals with $x = 0.3$ are synthesized by a floating zone techinque[18] and characterized by X-ray Laue as well as neutron diffraction experiments[18]. The crystals are subsequently cut, polished and annealed in an oxygen environment in preparation for pump–probe studies. In the pump–probe spectroscopy studies, $Pr_{0.7}Ca_{0.3}MnO_3$ samples at 30 K are excited by 200–300 fs, ~1 μJ pulses tuned in the mid-infrared spectral region around 17.5 μm (corresponding to a photon energy $h\nu = 71$ meV). The pump pulses are focused to a fluence of about 1 mJ cm^{-2} and the transient changes in reflectivity are probed by delayed femtosecond pulses at visible to near-infrared frequencies to identify the characteristic spectral signatures and formation time of the metallic phase. Figure 2a shows the transient reflectivity $\Delta R/R$ at 800 nm after impulsive vibrational excitation at 17.5 μm and compared with above-bandgap pulsed excitation. The reflectivity responses are identical, with large long-lived changes in reflectivity developing within 1 ps of excitation. Moreover, these changes exhibit threshold and saturation dependence on the pump fluence, characteristic of a phase transformation to the metallic state, as previously established for above-bandgap excitation[15].

Figure 2b shows the spectral dependence of the $\Delta R/R$ signal (at 1 ps delay) for the case of the 17.5 μm pump wavelength. The spectrum of the reflectivity changes exhibits identical features, as in previous optical studies in $Pr_{0.7}Ca_{0.3}MnO_3$ (ref. 17), which showed that the transition to the conducting phase (induced either by applied magnetic field, or by above-bandgap transient optical excitation) is characterized by decreased reflectivity at photon energies in the 0.5–1.9 eV range and increased reflectivity at higher photon energies. Such reflectivity changes have been interpreted as a consequence of melting of the charge order and of the collapse of the 0.3 eV insulating gap, leading to the formation of a pseudo plasma edge in the metallic state[12]. Our observation of the ultrafast formation of a metallic-like reflectivity spectrum after 17.5 μm pump excitation provides evidence that the metallic state is formed promptly (within the 300 fs experimental resolution) via direct vibrational excitation, and that this state persists for hundreds of picoseconds. Although the spectral reflectivity signature is associated with the conducting phase of $Pr_{0.7}Ca_{0.3}MnO_3$, our recent measurements show that this is not uniquely indicative of the melting of charge order, because a similar spectral signature is observed when the metallic phase is induced by photoexcitation from the room-temperature paramagnetic insulating phase.

Figure 2c shows the dependence of the reflectivity change (measured at 1 ps delay, 800 nm probe wavelength) on the pump wavelength, in the vicinity of the phonon resonance. The observed reflectivity change clearly vanishes when the pump wavelength is tuned outside the 17.5 μm phonon absorption band. The magnitude of $\Delta R/R$ is maximum when the excitation wavelength is resonant with the Mn–O stretching mode, providing further evidence of an ultrafast vibrationally induced phase transition. The linear absorption spectrum around the 17.5 μm phonon resonance is not polarization-dependent[12] and no significant dependence on the pump polarization was observed either in the pump–probe experiments or in the conductivity measurements.

In addition to the optical measurements, changes in the sample conductivity are directly monitored by measuring the transient sample resistance after mid-infrared excitation. Gold electrodes with a 200-μm-wide gap are vacuum-evaporated onto the sample surface[2], and are d.c.-biased at 30 V. Measurements are performed at 30 K, where the charge-ordered, anti-ferromagnetic phase exhibits strong insulating character[8]. Laser pulses at 17.5 μm are used to excite the sample (under conditions identical to those described above), with the laser spot fully covering the space between the electrodes. The current flowing through the sample was monitored by measuring the voltage drop across a 50 Ω resistor. Mid-infrared excitation results in a dramatic 1,000-fold increase in current (Fig. 3, upper panel), corresponding to a resistance drop from 2 GΩ to 1.25 MΩ. The high conductivity state develops within the 4-ns resolution of the electronics and exhibits a resonance behaviour similar to that observed in the optical measurements (Fig. 2c). Figure 3 (lower panel) shows the increase in the sample conductivity derived from the measured transient resistance by assuming that the transition to the conductive state is uniform throughout the excited sample volume. Given the laser spot size at the electrodes (200×300 μm^2) and the penetration depth of the mid-infrared light (~0.5 μm)[12], the sample conductivity increase is estimated to exceed 10^5, from $\sim 3 \times 10^{-8}\,\Omega^{-1}\,\mathrm{cm}^{-1}$ to $\sim 5 \times 10^{-3}\,\Omega^{-1}\,\mathrm{cm}^{-1}$. The metastable metallic phase is formed and relaxes within the experimental time resolution of 4 ns. The precise assessment of the lifetime of the metallic phase by means of transport measurements is hindered by oscillations due to ringing in the fast current detection electronics with a time-dependent sample resistance (see Fig. 3). However, the sample recovers its original resistance

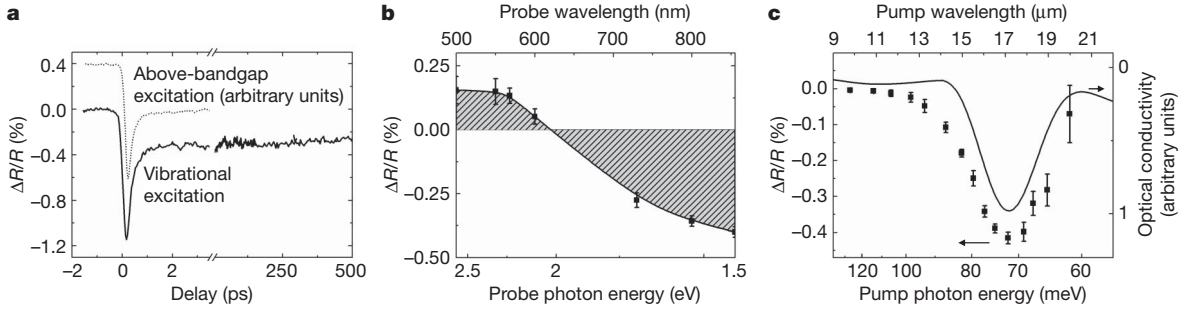

Figure 2 | Femtosecond pump–probe reflectivity studies. a, Relative change of reflectivity at 800 nm ($\Delta R/R$) as a function of pulse delay after vibrational excitation at 17.5 μm (solid line) and 800 nm photo-excitation (dotted line). **b**, Spectral dependence of $\Delta R/R$ measured 1 ps after vibrational excitation. The solid line is a spline fit to the data points (squares). The shift of spectral weight towards longer wavelengths, shown by the shaded area under the curve, is a signature of the formation of the metallic phase[12,15]. **c**, $\Delta R/R$ at 800 nm measured 1 ps after excitation (squares) and absorption spectrum around the 17.5 μm phonon resonance (solid line). For comparison, the phonon spectrum is convolved with the spectrum of the broad-bandwidth pump pulses. Error bars are s.d.

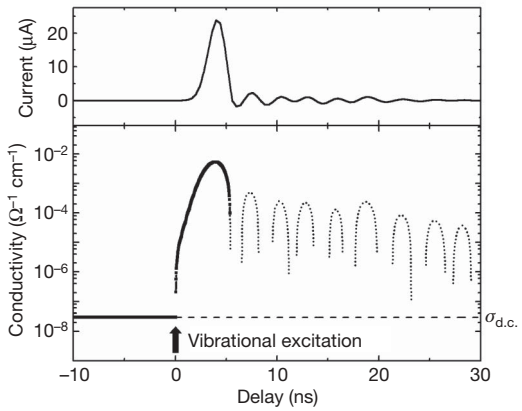

Figure 3 | Time-dependent transport measurement. Vibrational excitation of the Mn–O stretching mode results in a $\sim 10^3$ increase in the sample current (upper panel) and a corresponding $\sim 10^5$ increase in the sample conductivity (lower panel). The metastable metallic phase is formed and relaxes within the experimental time resolution of 4 ns. The current oscillations following the main pulse are due to electronic ringing and cannot be converted accurately into sample conductivity, so the derived conductivity oscillations are shown as a dotted line. The dashed line shows the d.c. conductivity of the insulating phase of $Pr_{0.7}Ca_{0.3}MnO_3$ at 30 K.

within several tens of nanoseconds. In these measurements, contributions from interband carrier excitations are negligible because five photons at 17.5 μm (71 meV) are required to span the 0.3-eV insulating bandgap of $Pr_{0.7}Ca_{0.3}MnO_3$ (ref. 12). The moderate temperature jump due to laser excitation (estimated at <2 K for excitation at the peak of the phonon resonance) can also be ruled out as the origin of the resistivity drop. As emphasized in the introduction, in $Pr_{0.7}Ca_{0.3}MnO_3$ an insulator-to-metal phase transition cannot be induced by temperature[8].

Our results clearly show that resonant excitation of the Mn–O phonon vibration in $Pr_{0.7}Ca_{0.3}MnO_3$ drives the system on a femtosecond timescale into a metastable, nanosecond-lived, high-conductivity phase. We note that this occurs in the electronic ground state of the solid and no electronic excitation is involved. These results strongly suggest that coherent modulation of the 'tolerance factor' gives rise to dramatic changes in the electron hopping probability, providing important new insight into the physics underlying the behaviour of this strongly correlated material.

Given the present limitations in generating mid-infrared pulses beyond 25 μm, it is not yet possible to assess the specificity of the Mn–O stretching vibration by comparing it with excitation of lower-frequency phonon modes, including the Mn–O–Mn bending mode, which is also likely to modulate the tolerance factor significantly. Moreover, an important role in inducing the phase transition and subsequently stabilizing the metallic phase may be played by ultrafast vibrational energy redistribution via anharmonic coupling to the Mn–O–Mn bend, or to other modes (for example, non-infrared-active Jahn–Teller modes[19]) that may also influence the electron localization and delocalization.

In future, experimental techniques such as magneto-optic Kerr effect spectroscopy or time-resolved photo-emission electron microscopy[20] will be important for probing the spin and magnetization dynamics after mid-infrared excitation. In a magnetoresistive manganite metallicity is associated with ferromagnetism through the double-exchange mechanism[21], so the formation of a metallic state implies the possibility of generating ferromagnetic domains on ultrafast timescales by excitation of specific vibrational degrees of freedom—a remarkable consequence of the strong coupling between magnetic, electronic and lattice degrees of freedom.

In summary, we have demonstrated the excitation of a specific phonon mode as a tool to drive the solid in the electronic ground state towards a competing phase of the system. The ultrafast vibrational control of correlated-electron phases is probably applicable in other interesting cases, opening a new window on their controversial physics and enabling time-resolved measurements under the unique conditions created by the initial localization of energy in specific vibrational modes. This approach may extend well beyond the case of colossal magnetoresistance manganites, providing new insight into the behaviour of complex matter, including the controversial nature of high-transition-temperature superconductivity and the role played by lattice vibrations in determining its electronic properties.

Received 5 May; accepted 23 July 2007.

1. Kiriukhin, V. *et al.* An X-ray induced insulator–metal transition in a magnetoresistive manganite. *Nature* **386,** 813–815 (1997).
2. Miyano, K. Tanaka, T. Tomioka, Y. & Tokura, Y. Photoinduced insulator-to-metal transition in a perovskite manganite. *Phys. Rev. Lett.* **78,** 4257–4260 (1997).
3. Fiebig, M. Miyano, K. Tomioka, Y. & Tokura, Y. Visualization of the local insulator-metal transition in $Pr_{0.7}Ca_{0.3}MnO_3$. *Science* **280,** 1925–1928 (1998).
4. Asamitsu, A. Tomioka, Y. Kuwahara, H. & Tokura, Y. Current switching of resistive states in magnetoresistive manganites. *Nature* **388,** 50–52 (1997).
5. Tokura, Y. *Colossal Magnetoresistive Oxides* Ch. 1 (Gordon & Breach Science Publishers, Amsterdam, 2000).
6. Dagotto, E. *Nanoscale Phase Separation and Colossal Magnetoresistance* Ch. 2–3 (Springer, Berlin/Heidelberg/New York, 2002).
7. Salamon, M. B. & Jaime, M. The physics of manganites: structure and transport. *Rev. Mod. Phys.* **73,** 583–628 (2001).
8. Tomioka, Y. Asamitsu, A. Kuwahara, H. & Moritomo, Y. Magnetic-field-induced metal-insulator phenomena in $Pr_{0.7}Ca_{0.3}MnO_3$ with controlled charge-ordering instability. *Phys. Rev. B* **53,** 1689–1692 (1996).
9. Anderson, P. W. & Hasegawa, H. Considerations on double exchange. *Phys. Rev.* **100,** 675–681 (1955).
10. Imada, M. Fujimori, A. & Tokura, Y. Metal-insulator transitions. *Rev. Mod. Phys.* **70,** 1039–1263 (1998).
11. Hwang, H. Y. Cheong, S-W. Radaelli, P. G., Marezio, M. & Batlogg, B. Lattice effects on the magnetoresistance in doped $LaMnO_3$. *Phys. Rev. Lett.* **75,** 914–917 (1995).
12. Okimoto, Y. Tomioka, Y. Onose, Y., Otsuka, Y. & Tokura, Y. Optical study of $Pr_{1-x}Ca_xMnO_3$ ($x=0.4$) in a magnetic field: Variation of electronic structure with charge ordering and disordering phase transitions. *Phys. Rev. B* **59,** 7401–7408 (1999).
13. Boris, A. V. *et al.* Infrared optical properties of $La_{0.7}Ca_{0.3}MnO_3$ epitaxial films. *J. Appl. Phys.* **81,** 5756–5758 (1997).
14. Ogawa, K. Wei, W. Miyano, K., Tomioka, Y. & Tokura, Y. Stability of a photoinduced insulator-metal transition in $Pr_{0.7}Ca_{0.3}MnO_3$. *Phys. Rev. B* **57,** R15033–R15036 (1998).
15. Fiebig, M. Miyano, K. Tomioka, Y. & Tokura, Y. Reflection spectroscopy on the photoinduced local metallic phase of $Pr_{0.7}Ca_{0.3}MnO_3$. *Appl. Phys. Lett.* **74,** 2310–2312 (1999).
16. Fiebig, M. Miyano, K. Satoh, T., Tomioka, Y. & Tokura, Y. Action spectra of the two-stage photoinduced insulator-metal transition in $Pr_{0.7}Ca_{0.3}MnO_3$. *Phys. Rev. B* **60,** 7944–7949 (1999).
17. Fiebig, M. Miyano, K. Tomioka, Y. & Tokura, Y. Sub-picosecond photo-induced melting of a charge-ordered state in a perovskite manganite. *Appl. Phys. B* **71,** 211–215 (2000).
18. Tomioka, Y. Asamitsu, A. Moritomo, Y. & Tokura, Y. Anomalous magnetotransport properties of $Pr_{1-x}Ca_xMnO_3$. *J. Phys. Soc. Jpn* **64,** 3626–3630 (1995).
19. Millis, A. J. Shraiman, B. I. & Mueller, R. Dynamic Jahn–Teller effect and colossal magnetoresistance in $La_{1-x}Sr_xMnO_3$. *Phys. Rev. Lett.* **77,** 175–178 (1996).
20. Choe, S.-B. *et al.* Vortex core-driven magnetization dynamics. *Science* **304,** 420–422 (2004).
21. Zener, C. Interaction between the *d*-shells in the transition metals. II. Ferromagnetic compounds of manganese with perovskite structure. *Phys. Rev.* **82,** 403–405 (1950).

Acknowledgements We thank Y. Okimoto for providing the optical conductivity spectra and S. Wall for help in the figures preparation. This work was supported by the Director, Office of Science, Office of Basic Energy Sciences, Materials Sciences and Engineering Division, of the US Department of Energy. Work at the University of Oxford, UK, was supported by the European Science Foundation through a European Young Investigator Award, and by the Oxford University Press through a John Fell Award.

Author Information Reprints and permissions information is available at www.nature.com/reprints. The authors declare no competing financial interests. Correspondence and requests for materials should be addressed to M.R. (mrini@lbl.gov) and to A.C. (a.cavalleri1@physics.ox.ac.uk).